

**CHE499 Directed Research Project
Final Report**

Simulation-based Design of Aeroponics Nutrient Distribution System
using multiphase CFD

Romrawin Chumpu

Department of Chemical Engineering
University of Waterloo
April 19, 2019

Abstract

New technology for growing plant, such as an aeroponic system, provides great advantages to the development of disease-free cultivation, nutrient-rich supply and higher quality of plant in the soil-less culture. This project aims to apply theoretical assumption, and engineering designs into computational fluid dynamic (CFD) simulation to study the multiphase flow models for aeroponic nutrient distribution. This study is focused on the geometry design of grow tray in commercial aeroponic system. Geometry simulation was generated by Gmsh program in a triangle shape with one gas input and two liquid/gas output on the opposite sides. OpenFoam software was used to simulate the multiphase flow behavior by using TwoPhaseEulerFoam solver. Simulation results show that CFD can be used to predict the behaviour of aeroponic system.

Contents

1	Introduction	2
1.1	Background	2
1.1.1	Aeroponic System	2
1.1.2	Types of Aeroponic System	4
1.1.3	Commercial Aeroponic System	4
1.2	Multiphase Model	6
1.3	Literature Review	6
2	Theory	8
2.0.1	Disperse Gas-Liquid Flows	8
2.0.2	Euler-Euler Approach	9
2.0.3	Governing Equations	10
3	Simulation	12
3.1	Geometry	12
3.1.1	Gmsh Software	12
3.2	Solver	14
3.2.1	OpenFOAM	14
4	Results and Discussion	15
4.1	Results and Discussions	15
5	Conclusion	19
5.1	Conclusion	19
5.2	Future Study	19
A	Appendix 1: Geometry Code by Gmsh and BlockMesh	21
A.1	Gmsh code	21
A.2	BlockMesh code	24
	References	31

Chapter 1

Introduction

1.1 Background

1.1.1 Aeroponic System

Aeroponic system is a process of suspending plant in the air and mist environment. Without soil as a base of growing medium, a plant needs to receive an adequate amount of nutrient from nearby or attachable surface to sustain plant growth [Raviv and Lieth2008]. A highlight of this system includes spraying nutrient-rich solution to the dangling root where the solution moves toward between environment and roots surface in close or semi-closed area as shown in Figure 1.1.



Figure 1.1: Aeroponic system environment [Raviv and Lieth2008]

One advantage of the aeroponic system is that the plant is kept away from the soil, prevention contracting to pathogens and diseases, which makes the plant grow healthier than in the soil. Under the aeroponic grow tray, one hundred percent of root surface exposes to the air. Osmosis of nutrient solution is proportional to the increased contact surface area. Ideally, plant roots would have the highest potential of accessing pure water, oxygen exchange and disease-free cultivation, if sufficient nutrient solution is applied. Moreover, full access to oxygen and carbon dioxide could be a huge support to the generation of the plant in a natural manner for successful physiological development.

The main four components of aeroponic structure consists of mist generation equipment such as misters, sprayers, or other devices. In the system, root aeration is optimized, which is the main advantage leading to a plant performance increase as compared in soil medium. In a closed-system, they provide a diffused micro-droplet environment to sustain constant behavior air circulation unit. Since nutrient droplet is vital for sustaining aeroponic growth, if the droplet is too large, oxygen would not be able to access the root surface, and then the plant will be overwhelming in hypotonic condition. On the other hand, if the droplet is too fine, the plant root would not develop a lateral behavior [Stoner and Clawson1998]. Despite the excessive use of pump, in traditional method can produce irreversible damages according to the losses of power.



Figure 1.2: Aeroponic grow tray

1.1.2 Types of Aeroponic System

Low-pressure aeroponics

In a low-pressure aeroponic system, grow tray that contains the plant are placed above storage of nutrient solution. The nutrient solution is delivered to the grow tray by a low-pressure pump, which then the droplet are collapsed and flow back the liquid at the bottom of the grow tray to the storage. This type provides too fine nutrient droplet in the unit. The plant suffers from a dry section of the root system which is prevented adequate nutrient to roots surface.

High-pressure aeroponics

High-pressure aeroponics structure is closely similar to low-pressure aeroponic, but the mist is generated from the high-pressure pump. This high-pressure pump provides nutrients micro-droplets size 20-50 μm delivered to the grow tray. This size of the droplet is required because an adequate supply of nutrient to the root system is presented. Therefore, most high-pressure aeroponics includes new technologies for developing water purification, nutrient reuptake sterilization in the delivery system.

1.1.3 Commercial Aeroponic System

The aeroponic system is developing in many commercial companies such as AeroFlo (1.3), Aero Farm Systems, Neofarms, etc. High-pressure devices are used in controls system because it provides the appropriate size of the droplet. Each company has its feature aeroponic product, which aims to extend plant growing performance.

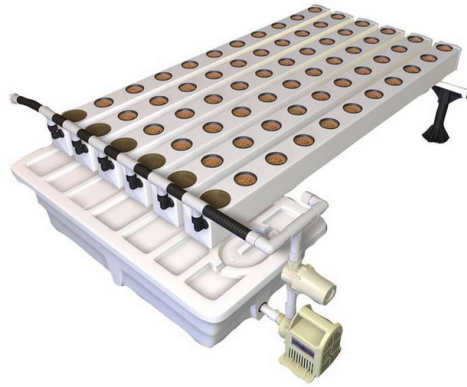


Figure 1.3: General Hydroponics AeroFlo 60 Site Aeroponic System*

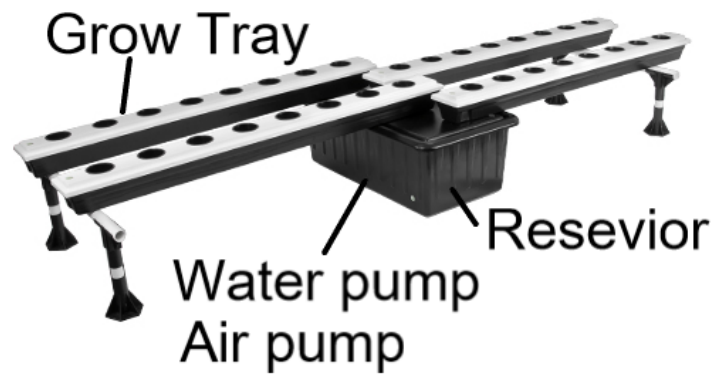


Figure 1.4: General commercial aeroponic system component

A general commercial prototype of the aeroponic system consists of four components: water pump, air pump, reservoir, and grow tray.

In general consideration of engineering design, we would focus on the feasibility and geometry of grow tray that would have an effect on the multiphase

flow dynamic by the technique of computational fluid dynamic (CFD).

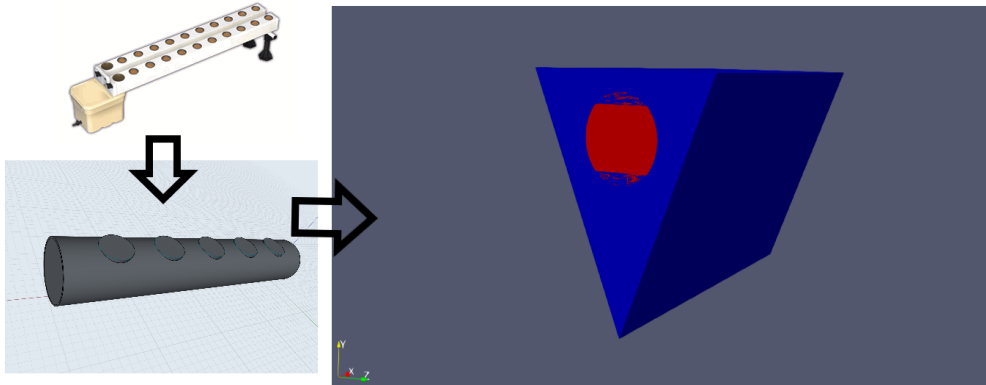


Figure 1.5: Developing commercial prototype to simulation geometry

1.2 Multiphase Model

Multiphase flow is the term which generally uses to assign phenomena of fluid flow consisting of two or more phases. Whereas in the mixing phases are assumed well-mixed, and some level of phases are separated above the molecular level. Mixing phase could be classified according to the state of different phases as following, gas-solid, liquid-solid, and gas-liquid flows. In this project, gas-liquid flow is introduced to simulate the aeroponic system [Garcia et al.2005].

1.3 Literature Review

Many aspects of the aeroponic system started from aiming to avoid using soil as a medium, and produce high quality of the plant. Specifically, each plant has an optimal nutritional solution requirement in an aeroponic environment which has a relation with the required unit components and scaling design. Size and number of the tube affect the system. Tessema et al., showed that the number of small tubes was not significantly affected to nutrition distribution. Large and medium tubes were significantly affected nutrition distribution based on a number of the tube. Therefore, in our simulation, we would possibly compare the number of the tube between the manifold and one direction pathway [Tessema et al.2017].

Plant growth depends on a gas exchange between the contact surface. Air circulation in the unit system contains approximately 21% of oxygen. Measurement of oxygen flow in a closed system was studied to root atmosphere condition [Moez et al.2001, Asao2012]. Results show the different response of the plant, and maintain growth in stressful conditions. Among all approaches, the aeroponic system is presented as the most adequate system [Asao2012]. Special care should be taken for an adequate and continuous aeration flow. Also, mass transfer limitation, especially of oxygen, could be significantly reduced or eliminated by using a gas-phase culture system [Towler et al.2008, Moez et al.2001].

Design and development and application of aeroponic technology has been developed for decreasing stress conditions, drought stresses, pathogenic effects, and overall plant morphology and physiology. Grow tray unit is one of the challenges in liquid-gas phase flow. Because the system needs to be controlled delivering nutrient solution droplet to the submerged tissues as in the gas-phase surrounding [Towler et al.2008]. Droplet sizes for mists are ranged from 0.01-10 μ m [Perry and Green1997, Towler et al.2008].

Plant tissue is highly sensitive to the gas-phase environment, especially O_2 , CO_2 , and ethylene. Suspended root attaches a full contract to the aeroponics system. Attempting to increase gas transport by increasing the size or number of the bubble can damage the shear-sensitive of plant tissues [Towler et al.2008]. The optimum condition should be investigated by further research. If the nutrient solution in a gas composition is manipulated in the unit, the ability to grow plant based on gas exchange rate would also increase.

Large scale integration of aeroponics was studied in the Institute of Biotechnology at the Vietnam National University of Agriculture. Their works have shown that aeroponic agricultural technology has significantly improved Vietnam's potato production. The aeroponic approach in Vietnam will begin to be more accessible as a low cost, disease-free cultivation, which helps local framers effort the high quality of commercial potatoes [Spinoff2006].

Chapter 2

Theory

2.0.1 Disperse Gas-Liquid Flows

In general topology of multiphase flow, *disperse flows* means the flows which one phase behaves like discrete elements consisting of finite particles such as droplet or bubble. Discrete elements are not connected to each other as in the same mixing regime.

First definition of the two-phase model is *volumetric fraction* shown individual components of two phases. α_l, α_g are defined as a volumetric fraction of liquid phase and gas phase respectively as the subscripts shown on the right side of the alpha symbol. By the assumption of a two-phase model.

$$\alpha_l + \alpha_g = 1 \quad (2.1)$$

Volumetric fluxes, j_l, j_g meaning to the volumetric flow per unit area of individual components will be added to the *total volumetric flux*, j_i , where i refers to x, y and z dimensional flows.

$$j_i = j_{li} + j_{gi} + \dots = \sum_N j_N \quad (2.2)$$

N in equation 2.2 refers to the properties of specific phase (l is denoted as liquid phase and g is denoted as gas phase).

Velocities of individual phases are denoted by u_l, u_g and the slip velocity between the two phases is denoted by u_{AB_i} . Therefore,

$$u_{AB_i} = u_{li} - u_{gi} \quad (2.3)$$

Provided definitions for finite volume of the flow, the *volumetric flux* of each component by the function of volumetric fraction and velocity could be derived by

$$\dot{j}_i = \alpha_l u_{l_i} \quad (2.4)$$

$$\dot{j}_{g_i} = \alpha_g u_{g_i} \quad (2.5)$$

and the relation derives of the as

$$\dot{j}_i = \alpha_l u_{l_i} + \alpha_g u_{g_i} + \dots = \sum_N \alpha_N u_{N_i} \quad (2.6)$$

Equation 2.6 clearly shows a property of multiphase mixture goes into one finite volume by assuming in a unit cube with parallel edges along i direction. Determining another property directly related to describe the amount of mass per unit volume, the mixture density, denoted by ρ and the relation to both phases shown as

$$\rho = \sum_N \alpha_N \rho_N \quad (2.7)$$

Density of each component could be calculated to one important property, *Massfluxes*, denoted by G_i . Therefore, the mass flux of the liquid and gas phase could be derived as a function of density and volumetric flux as following.

$$G_{l_i} = \rho_l \dot{j}_{l_i}; G_{g_i} = \rho_g \dot{j}_{g_i} \quad (2.8)$$

$$G_i = \sum_N \rho_N \dot{j}_{N_i} \quad (2.9)$$

All specific properties are introduced in this section, including notations that will be used throughout the report. This basic notation leads to the derivation of mass, momentum and energy equations in the next following sections.

2.0.2 Euler-Euler Approach

In the Euler-Euler approach (EE), the two phases are treated mathematically as interpenetrating continuous flow. The concept of phasic volume fraction is applied due to the volume of the phase could not be occupied by the other phase [Garcia et al.2005, Brennen2005]. These volume fractions are assumed to be continuous functions of space and time, the sum is equal to one as in equation 2.1. The conservation of each phase are obtained and discussed in section 2.0.3. These equations are closed by providing constitutive relations which are obtained from empirical formation. As a consequence, EE approach is applied in OpenFOAM TwoPhaseEulerFoam solver in the section 3.2.1.

2.0.3 Governing Equations

Mass Equations

Mass flow of liquid and gas through the perpendicular face in i direction subtracts to its outflow from the assumed finite volume are referred to the *net* of mass transport. Assuming that the net of the mass of component is tiny, divergence function applies to the value

$$\frac{\partial(\rho_l j_{l_i})}{\partial x_i} \quad (2.10)$$

$$\frac{\partial(\rho_g j_{g_i})}{\partial x_i} \quad (2.11)$$

Equation 2.10 and 2.11 also refer to the increased rate of mass transfer in the assumed finite volume. Therefore, the *conservation of mass* in two-phase flow is calculated by

$$\frac{\partial}{\partial t}(\rho_l \alpha_l) + \frac{\partial(\rho_l j_{l_i})}{\partial x_i} = R_l \quad (2.12)$$

$$\frac{\partial}{\partial t}(\rho_g \alpha_g) + \frac{\partial(\rho_g j_{g_i})}{\partial x_i} = R_g \quad (2.13)$$

Where R_N is the rate of mass transfer from the other phases per unit total volume, called *mass interaction terms*.

The sum of the conservation of mass in all dimensions provides the combined *mass continuity equation* or *Navier-Stokes equation* as a function of component density over time and the movement of mass transport in all direction at certain control volume.

$$\frac{\partial}{\partial t}(\rho_N \alpha_N) + \nabla(\alpha_N \rho_N \vec{u}_N) = R_N \quad (2.14)$$

Conservation of mass could be applied to the conservation of the number of bubble in the disperse flow. Assuming steady state condition as the state that the number of bubble is constant within the control volume.

$$\frac{\partial n_l}{\partial t} + \frac{\partial(\rho_l j_{l_i})}{\partial x_i} = 0 \quad (2.15)$$

Where n_l is the number of droplet per unit total volume.

In the control volume, define droplet volume as v_l . Then, the volumetric fraction of liquid phase could also imply by

$$\alpha_l = n_l v_l \quad (2.16)$$

Substituting equation 2.16 into 2.14 obtains

$$\frac{\partial}{\partial t}(\rho_l n_g v_l) + \nabla(n_l v_l \rho_l \vec{u}_l) = R_l \quad (2.17)$$

The equation 2.17 implies that the mass fraction changes with respect to time. The velocity and mass changes with respect to all direction in control volume.

Solving for the relation of R_l using equation 2.15 obtains

$$R_l = n_l \left(\frac{\partial(\rho_l v_l)}{\partial t} + u_{ly} \frac{\partial(\rho_l v_l)}{\partial x_i} \right) = n_l \frac{D_l}{D_l t}(\rho_l v_l) \quad (2.18)$$

Where $D_g/D_g t$ is the Lagrangian derivative of the disperse phase.

From equation 2.18, the rate of mass transfer of liquid phase per number of droplet equal to the Lagrangian rate of mass of each droplet over the time.

Momentum Equations

Continuing equation is implied by differential equations. In the same control volume, the flux of momentum of liquid phase can be determined by

$$f_{l_i} = \rho_N j_{l_i} \vec{u}_{l_k} \quad (2.19)$$

Therefore, the net flux of momentum in finite volume is

$$\frac{\partial(\rho_l \alpha_l \vec{u}_{l_i} \vec{u}_{l_k})}{\partial x_i} \quad (2.20)$$

From this relation, the force in k direction of the liquid phase is calculated by

$$F_{l_k} = \frac{\partial}{\partial t}(\rho_l \alpha_l \vec{u}_{l_i}) + \frac{\partial}{\partial x_i}(\rho_l \alpha_l \vec{u}_{l_i} \vec{u}_{l_k}) \quad (2.21)$$

This is the difficulty of the momentum conservation to completely construct the forces function F_{l_k} . This term should include the individual force acting within elementary volume, the pressure, viscous stresses, and the interaction forces between two phases. The derivation of this term would rather conduct in further study.

Chapter 3

Simulation

3.1 Geometry

3.1.1 Gmsh Software

Gmsh is one of free softwares for finite element mesh generator which provide meshing tool with advanced visualization capability. Gmsh allows user specify their own geometry by either using parametric input to generated module or the graphical user interface, and stored in *.geo* suffix ASCII text file.

In this project, we generate the triangle shape grow tray with one gas inlet, and two gas/liquid outlets. Gmsh code in *.geo* format is shown in A.1.

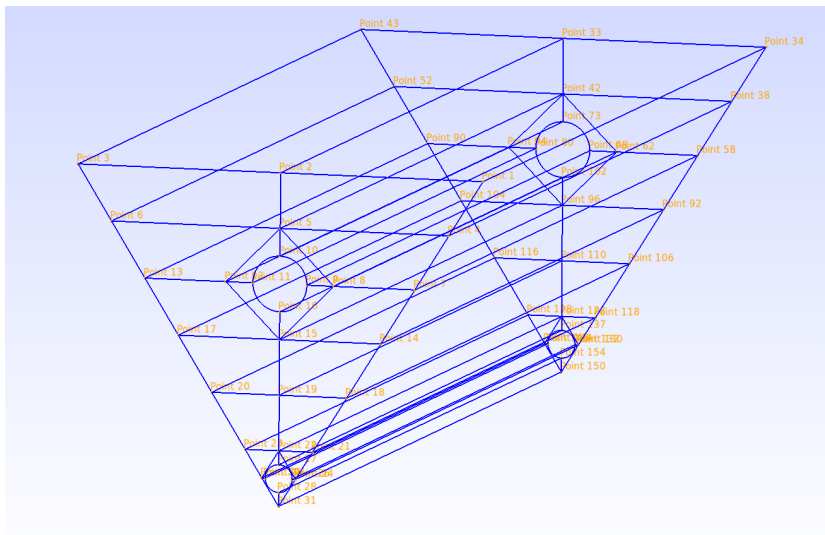


Figure 3.1: Gmsh triangle shape grow tray

From figure 3.1, we set the scale of geometry as follow:

- Length (l) = 50 cm
- Height (h) = 16 cm
- Top-width ($2w$) = 20 cm

The scale also define as these variable in code A.1.

After all points, lines, surface, and volume are defined and connected, then the mesh of geometry could be successfully generated within Gmsh fuction.

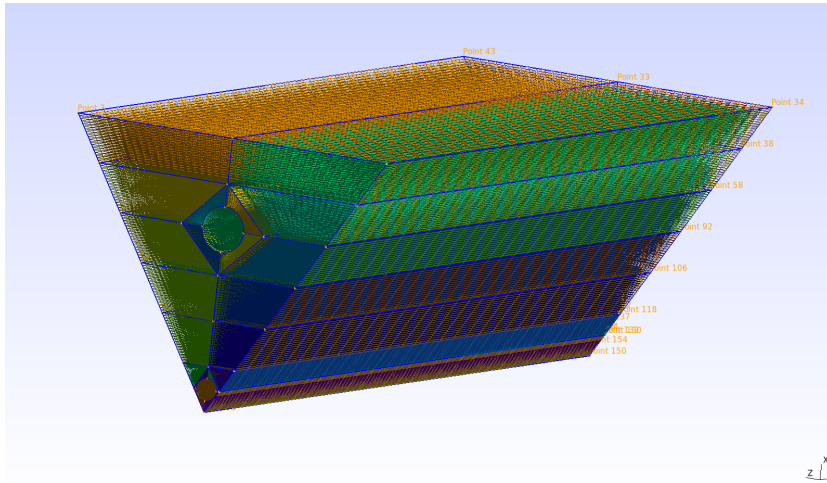


Figure 3.2: Meshing triangle grow tray

Therefore, the mesh of geometry is visualized as in Figure 3.2. The file can be extracted as the suffix *.msh* file, and ready to analyze by CFD. CFD solving approach will be discussed in the next section.

3.2 Solver

3.2.1 OpenFOAM

TwoPhaseEulerFoam

Two incompressible fluid phases with one dispersed phase are solved using this solver. Both the phases are described using the Eulerian conservation equations and thus it is referred as Euler-Euler model. Each of the phases are treated as a continuum in this approach.

The momentum transfer is determined from the instantaneous forces acting on the dispersed phase, comprising drag, lift and virtual mass. These forces are phase fraction dependent.

The conservation equations are discretised using the finite-volume method and solved in a solution procedure, which is based on the PISO algorithm, and adapted to the solution of the two-fluid model

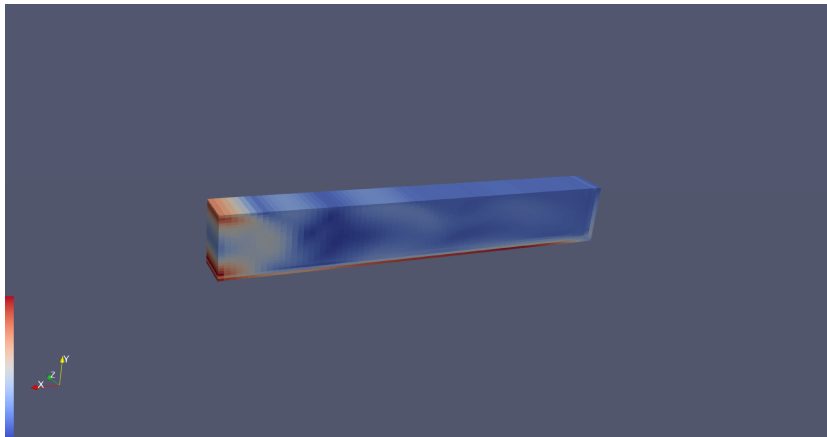


Figure 3.3: Example of contour TwophaseEulerFoam in rectangle geometry

Chapter 4

Results and Discussion

4.1 Results and Discussions

After running simulation in OpenFOAM, the results are shown as Figure 4.1 to 4.7 below.

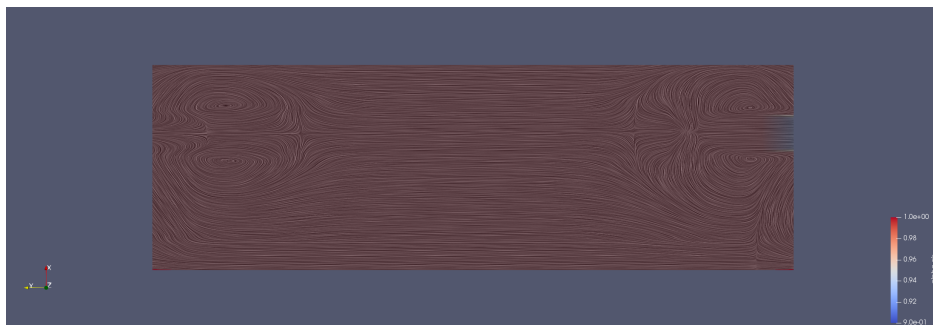


Figure 4.1: Aeroptic simulation result at time step = 1 second

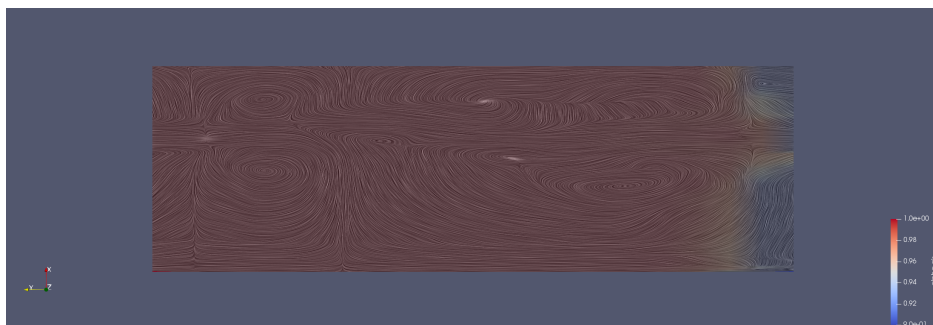


Figure 4.2: Aeroptic simulation result at time step = 5 second

Contour line of simulation result was visualized based on the volume fraction of the air at $\alpha_g = 1$ shown as the red part of middle cross-sectional rectangular shape. The blue part implies to the volume fraction of air $\alpha_g = 0$, marked in the legend at the right bottom of figure 4.1. The steam line in Figure 4.1 shows the mixing phase including partial of droplet gradually flows at the gas input surface (the right side of rectangular). We set the flow at the -y direction, which means the flow is coming toward the input at right side flowing to the output at left side of the geometry. Inside the geometry, the gas phase or air aeration is moving in the pattern of flow dispersion with two vortices above and below at input/output surfaces. When the droplet slowly flow in, the gas phase faces shear stress from the other phase, and push the small contained volume perpendicularly against the force due to the momentum equation as in the term F_{l_k} equation 2.21. This also can imply to Lagrange equation 2.17, vortex simulation of air phase distribution provide low level of organization presented in the second term of directional flow.

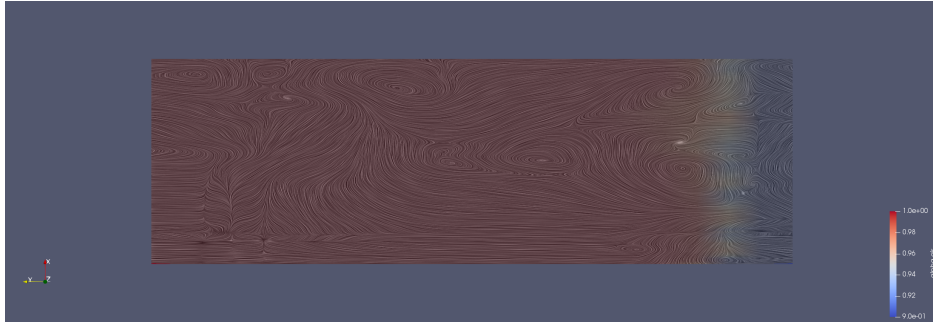


Figure 4.3: Aeroponic simulation result at time step = 10 second

At the time step = 10 second, the simulation shows that the liquid phase gradually flow in, and is distributed along lateral axis before moving along the horizontal axis. The more vortices occurred along the geometry with the more likely elliptical shape of steam line than at the time step = 1 second. Because the more two phase interaction occurred as the R_l term in equation 2.17. The shear force and pressure between two phases are collided more, making the more less organization in the geometry due to the increase magnitude of particle dispersion. This is the sign of a good distribution of the aeroponic system, because the more turbulence vortices, the more distribution of the flow with in the unit. The droplet will be more accessible attached to the plant root where it is hanged above the grow tray.

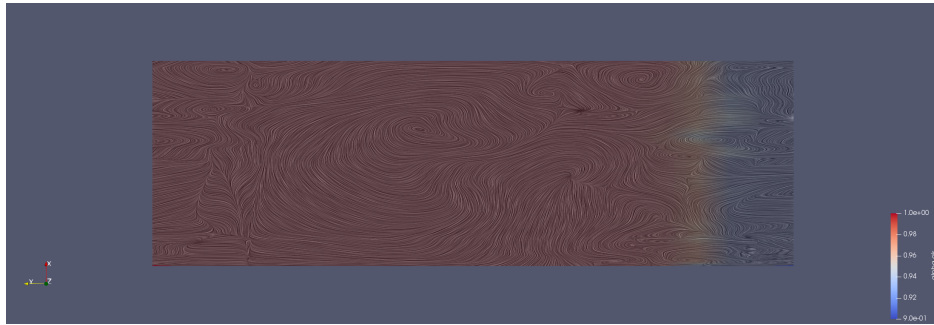


Figure 4.4: Aeroaponic simulation result at time step = 15 second

As shown the multiphase flow of the control unit at the time step = 15 to 35 second. The chaotic shape of steam line occurred at the interacted surface between liquid and gas phase at the geometry as shown in figure 4.4 to 4.7.

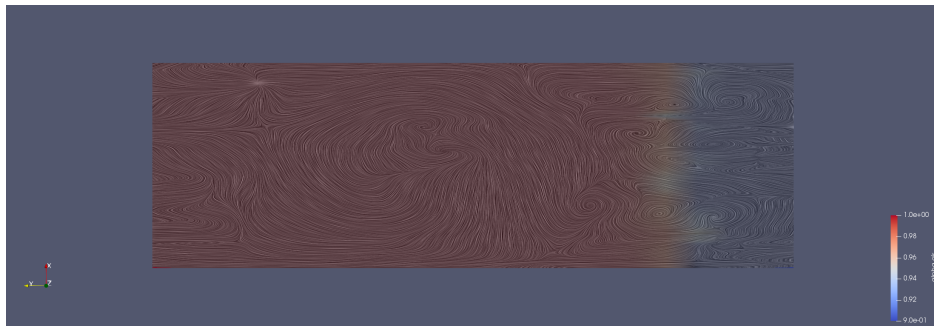


Figure 4.5: Aeroaponic simulation result at time step = 20 second

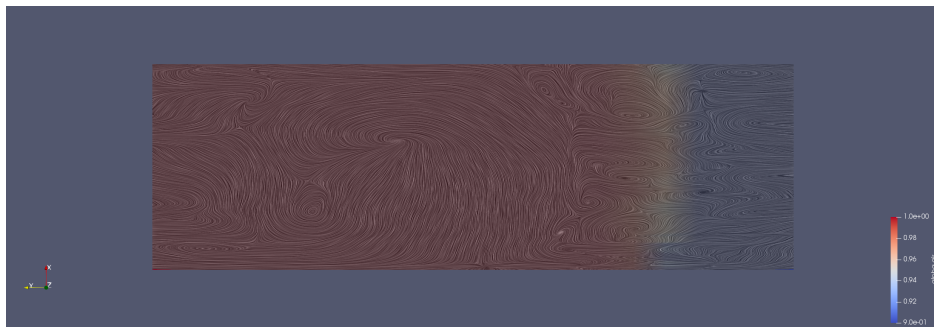


Figure 4.6: Aeroaponic simulation result at time step = 25 second

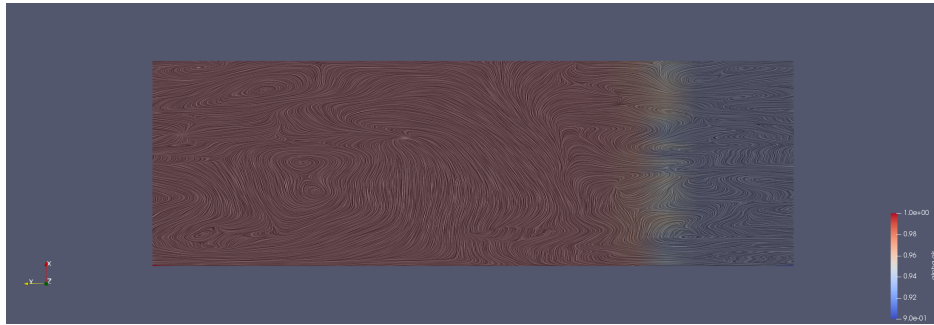


Figure 4.7: Aeroptic simulation result at time step = 30 second

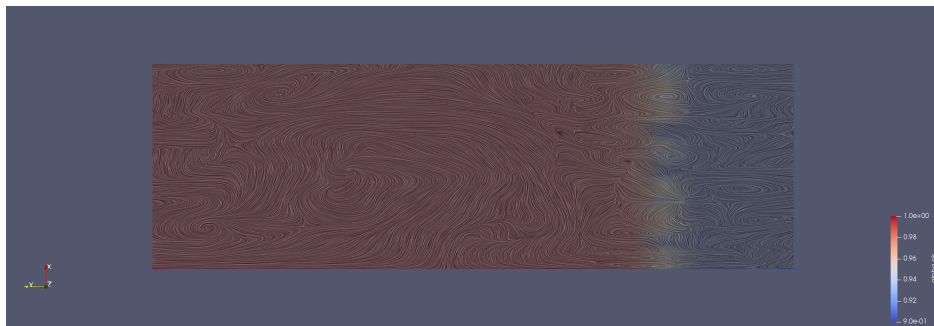


Figure 4.8: Aeroptic simulation result at time step = 35 second

As observation from figure 4.1 to 4.8, the blue that represent the volume fraction of liquid droplet has been flowed into the geometry. The stream line at that area shows turbulent like scheme regarding to dispersed flow behavior. Supporting from the Navier-Stokes equation 2.14, the function corresponds to the density, volumetric fraction, and velocity with respect to time and dimension. If one phase interacts to each other, the conservation of mass drives dispersed phase to have smaller vortexes, chaotic turbulent flow in between two phase interaction as shown in figure 4.4 to 4.8. The more chaotic, like eddies, at the initial part of distributed liquid input supports to the more droplet moving toward to the plant root surface.

The simulation result can produce the reasonable configuration of the multiphase flow. This result implies that the basic simulated flow could be a prior prediction of aeroponic distributed system.

Chapter 5

Conclusion

5.1 Conclusion

This project aimed to apply CFD simulation to engineering design. We gathered the information from background, literature review to analyze to the optimum condition of aeroponic simulation. Inspiring from a commercial prototype, a grow tray component was used to determine the dynamic properties of multiphase flow in the control system. Results of simulation show the system can be performed computer-based to prior predict behavior of the system. Comparison of actual fluid flow and simulation will be conducted in the future study.

5.2 Future Study

In this project, we also conduct the laboratory grow tray experiment along with CFD simulation as shown in Figure 5.1 and 5.2. The experiment will test on real plants, then, study the behavior of multiphase flow in actual environment conditions to the effect of the ability of plant growth.



Figure 5.1: Landscape view of laboratory aeroponic equipment



Figure 5.2: laboratory aeroponic equipment

Appendix A

Appendix 1: Geometry Code by Gmsh and BlockMesh

A.1 Gmsh code

```
// Gmsh project created on Mon Mar 22 00:41:36 2019
//+
lc = 1e-2;
//Mesh.ScaleFactor = 0.01; // Define mesh in centimeter scale

//Define variables
l = 50; //length
h = 16; //height
w = 10; //half-width
ir = h/12; //inlet radius
or = h/24; // outlet radius
n_surf = 20;
n_layers = 30;

//Points
Point(1) = {h, 0, -w, lc};
Point(2) = {h, 0, 0, lc};
Point(3) = {h, 0, w, lc};
Point(4) = {(5*h/6), 0, -(5*w/6), lc};
Point(5) = {(5*h/6), 0, 0, lc};
Point(6) = {(5*h/6), 0, (5*w/6), lc};
Point(7) = {(4*h/6), 0, -(4*w/6), lc};
Point(8) = {(4*h/6), 0, -(h/6), lc};
```

```

Point(9) = {(4*h/6), 0, -(ir), lc};
Point(10) = {(4*h/6)+(ir), 0, 0, lc};
Point(11) = {(4*h/6), 0, (ir), lc};
Point(12) = {(4*h/6), 0, (h/6), lc};
Point(13) = {(4*h/6), 0, (4*w/6), lc};
Point(14) = {(3*h/6), 0, -(3*w/6), lc};
Point(15) = {(3*h/6), 0, 0, lc};
Point(16) = {(4*h/6)-(ir), 0, 0, lc};
Point(17) = {(3*h/6), 0, (3*w/6), lc};
Point(18) = {(2*h/6), 0, -(2*w/6), lc};
Point(19) = {(2*h/6), 0, 0, lc};
Point(20) = {(2*h/6), 0, (2*w/6), lc};
Point(21) = {(h/6), 0, -(w/6), lc};
Point(22) = {(h/6), 0, 0, lc};
Point(23) = {(h/6), 0, (w/6), lc};
Point(24) = {(h/12), 0, -(w/12), lc};
Point(25) = {(h/12), 0, (or), lc};
Point(26) = {(h/12), 0, -(or), lc};
Point(27) = {(h/12)+(or), 0, 0, lc};
Point(28) = {(h/12)-(or), 0, 0, lc};
Point(29) = {(h/12), 0, (w/12), lc};
Point(30) = {(h/12), 0, 0, lc};
Point(31) = {0, 0, 0, lc};
Point(32) = {(4*h/6), 0, 0, lc};

```

//Lines

```

Line(1) = {1, 2}; Line(2) = {2, 3};
Line(3) = {1, 4}; Line(4) = {4, 5};
Line(5) = {2, 5}; Line(6) = {5, 6};
Line(7) = {3, 6}; Line(8) = {4, 7};
Line(9) = {7, 8}; Line(10) = {5, 8};
Line(11) = {8, 9}; Line(12) = {5, 10};
Line(13) = {5, 12}; Line(14) = {11, 12};
Line(15) = {12, 13}; Line(16) = {6, 13};
Line(17) = {7, 14}; Line(18) = {14, 15};
Line(19) = {15, 8}; Line(20) = {16, 15};
Line(21) = {15, 12}; Line(22) = {15, 17};
Line(23) = {13, 17}; Line(24) = {14, 18};
Line(25) = {18, 19}; Line(26) = {15, 19};
Line(27) = {19, 20}; Line(28) = {17, 20};
Line(29) = {18, 21}; Line(30) = {21, 22};

```

Line(31) = {19, 22}; Line(32) = {22, 23};
 Line(33) = {20, 23}; Line(34) = {21, 24};
 Line(35) = {24, 26}; Line(36) = {22, 27};
 Line(37) = {22, 24}; Line(38) = {22, 29};
 Line(39) = {25, 29}; Line(40) = {23, 29};
 Line(41) = {24, 31}; Line(42) = {29, 31};
 Line(43) = {28, 31};

//Circle

Circle(44) = {9, 32, 10};
 Circle(45) = {10, 32, 11};
 Circle(46) = {9, 32, 16};
 Circle(47) = {16, 32, 11};
 Circle(48) = {26, 30, 27};
 Circle(49) = {27, 30, 25};
 Circle(50) = {26, 30, 28};
 Circle(51) = {28, 30, 25};

//Curve and Surface

Curve Loop(1) = {-1, 3, 4, -5}; Plane Surface(1) = {1};
 Curve Loop(2) = {-2, 5, 6, -7}; Plane Surface(2) = {2};
 Curve Loop(3) = {-4, 8, 9, -10}; Plane Surface(3) = {3};
 Curve Loop(4) = {10, 11, 44, -12}; Plane Surface(4) = {4};
 Curve Loop(5) = {12, 45, 14, -13}; Plane Surface(5) = {5};
 Curve Loop(6) = {13, 15, -16, -6}; Plane Surface(6) = {6};
 Curve Loop(7) = {17, 18, 19, -9}; Plane Surface(7) = {7};
 Curve Loop(8) = {-19, -20, -46, -11}; Plane Surface(8) = {8};
 Curve Loop(9) = {20, 21, -14, -47}; Plane Surface(9) = {9};
 Curve Loop(10) = {22, -23, -15, -21}; Plane Surface(10) = {10};
 Curve Loop(11) = {24, 25, -26, -18}; Plane Surface(11) = {11};
 Curve Loop(12) = {26, 27, -28, -22}; Plane Surface(12) = {12};
 Curve Loop(13) = {29, 30, -31, -25}; Plane Surface(13) = {13};
 Curve Loop(14) = {31, 32, -33, -27}; Plane Surface(14) = {14};
 Curve Loop(15) = {34, -37, -30}; Plane Surface(15) = {15};
 Curve Loop(16) = {35, 48, -36, 37}; Plane Surface(16) = {16};
 Curve Loop(17) = {36, 49, 39, -38}; Plane Surface(17) = {17};
 Curve Loop(18) = {38, -40, -32}; Plane Surface(18) = {18};
 Curve Loop(19) = {41, -43, -50, -35}; Plane Surface(19) = {19};
 Curve Loop(20) = {43, -42, -39, -51}; Plane Surface(20) = {20};

//Circle

```

Curve Loop(21) = {-44, 46, 47, -45}; Plane Surface(21) = {21};
Curve Loop(22) = {-48, 50, 51, -49}; Plane Surface(22) = {22};

//Transfinite
Transfinite Curve{1:51} = n_surf;
Transfinite Surface{1:22};
Recombine Surface{1:22};

//Extrude surface
Extrude {0,1,0} {
  Surface{1:22}; Layers{n_layers}; Recombine;
}

//Define Physical groups
Mesh.Smoothing = 20;
Mesh.CharacteristicLengthMax = 1;
Geometry.PointNumbers = 1;
Geometry.Color.Points = Orange;
Geometry.Color.Volumes = Blue;
General.Color.Text = Black;

Physical Surface("gas_inlet") = {21} ;
Physical Surface("gas_outlet") = {507} ;
Physical Surface("liquid_outlet") = {525};
Physical Surface("walls") = {2, 1, 6, 5, 4, 3, 7, 10,
12, 11, 13, 14, 22, 15, 19, 20, 17, 16, 18, 8, 9, 73,
95, 117, 183, 205, 271, 315, 249, 161, 139, 227, 498,
293, 359, 337, 437, 376, 476, 398, 420, 60, 64, 108,
192, 280, 324, 445, 367, 467, 432, 354, 310, 262, 178,
94, 82, 481, 459, 503, 472, 446};
Physical Volume("volume") = {2, 6, 5, 1, 4, 10, 9, 21,
3, 8, 7, 12, 11, 14, 13, 18, 17, 16, 22, 15, 20, 19};

```

A.2 BlockMesh code

```

// General m4 macros

changecom(//)changequote([,]) dnl>
define(calc, [esyscmd(perl -e 'use Math::Trig; print ($1)')]) dnl>
define(VCOUNT, 0)
define(vlabel, [[// ]Vertex $1 = VCOUNT define($1, VCOUNT)

```



```

(0 h4 ora)    vlabel(27)
(1 h3 ora)    vlabel(28)
(1 h3 -ora)   vlabel(29)
(1 h4 -ora)   vlabel(30)
(1 h4 ora)    vlabel(31)
//
(0 h4 -w4)    vlabel(32)
(0 h4 w4)     vlabel(33)
(1 h4 w4)     vlabel(34)
(1 h4 -w4)    vlabel(35)
(0 0 0)      vlabel(36)
(1 0 0)      vlabel(37)
);

blocks
(
  //block0
  hex (5 1 3 7 4 0 2 6)(Nl Nh Nw) simpleGrading (1 1 1)
  //block1
  hex (16 17 6 4 10 14 13 9)(Nl Nh Nw) simpleGrading (1 1 1)
  //block2
  hex (10 14 13 9 11 15 12 8)(Nl Nh Nw) simpleGrading (1 1 1)
  //block3
  hex (11 15 12 8 18 19 7 5 )(Nl Nh Nw) simpleGrading (1 1 1)
  //block4
  hex (20 23 17 16 21 22 19 18)(Nl Nh Nw) simpleGrading (1 1 1)
  //block5
  hex (32 35 23 20 26 30 29 25)(Nl Nh Nw) simpleGrading (1 1 1)
  //block6
  hex (26 30 29 25 27 31 28 24)(Nl Nh Nw) simpleGrading (1 1 1)
  //block7
  hex (27 31 28 24 33 34 22 21)(Nl Nh Nw) simpleGrading (1 1 1)
  //block8
  hex (36 37 35 32 36 37 34 33)(Nl Nh Nw) simpleGrading (1 1 1)
);

edges
(
  //inlet
  arc 8 9 (0 h_arc_inlet 0)
  arc 9 10 (0 h2_arc_inlet -w_arc_inlet)
);

```

```

arc 10 11 (0 h1_arc_inlet 0)
arc 11 8 (0 h2_arc_inlet w_arc_inlet)
//outlet
arc 28 29 (1 h_arc_outlet 0)
arc 29 30 (1 h2_arc_outlet -w_arc_outlet)
arc 30 31 (1 h1_arc_outlet 0)
arc 31 28 (1 h2_arc_outlet w_arc_outlet)
);

```

boundary

```

(
  inlet
  {
    type patch;
    faces
    (
      (8 9 10 11)
    );
  }

  outlet
  {
    type patch;
    faces
    (
      (28 29 30 31)
    );
  }

```

walls

```

{
  type wall;
  faces
  (
    (3 1 5 7)
    (2 0 1 3)
    (4 6 2 0)
    (19 7 5 18)
    (22 19 18 21)
    (34 22 21 33)
    (36 37 34 33)
  )

```

```

(17 6 4 16)
(20 23 17 16)
(32 35 23 20)
(36 37 35 32)
(4 5 1 0)
(16 10 9 4)
(11 18 5 8)
(20 21 18 16)
(32 26 25 20)
(27 33 21 24)
(36 36 33 32)
(26 27 24 25)
(2 6 7 3)
(17 14 13 6)
(15 19 7 12)
(15 12 13 14)
(23 22 19 17)
(35 30 29 23)
(31 34 22 28)
(37 37 34 35)
);
}
interfere
{
    type patch;
    faces
    (
        (4 9 13 6)
        (9 8 12 13)
        (8 5 7 12)
        (16 10 14 17)
        (10 11 14 15)
        (11 18 19 15)
        (20 23 29 25)
        (25 24 28 29)
        (24 21 22 28)
        (32 26 30 35)
        (26 27 31 30)
        (27 33 34 31)
        (16 18 19 17)
        (4 5 7 6)
    )
}

```

```
                (20 21 22 23)
                (32 33 34 35)
                (36 37 37 36)
            );
        }
    );
```

```
mergePatchPairs
(
);
```

References

- [Asao2012] Asao, T. (2012). *Hydroponics A Standard Methodology for Plant Biological Researches*. InTech.
- [Brennen2005] Brennen, C. E. (2005). *Fundamentals of Multiphase Flows*. Cambridge University Press 2005.
- [Garcia et al.2005] Garcia, M., Sommerer, Y., Schonfeld, T., and Poinso, T. (2005). Evaluation of euler-euler and euler-lagrange strategies for large-eddy simulations of turbulent reacting flows. *Open Access*.
- [Moez et al.2001] Moez, J., Drevon, J.-J., and Aouani, M. E. (2001). Effects of hydroponic culture system and nacl on interactions between common bean lines and native rhizobia from tunisian soils. *Agronomie*, 21.
- [Perry and Green1997] Perry, R. and Green, D. (1997). *Perry's Chemical Engineer's Handbook*. McGraw-Hill.
- [Raviv and Lieth2008] Raviv, M. and Lieth, J. H. (2008). *Soilless Culture*. ELSEVIER.
- [Spinoff2006] Spinoff, N. (2006). Progressive plant growing has business blooming. *Environmental and Agricultural Resources NASA Spinoff 2006*.
- [Stoner and Clawson1998] Stoner, R. and Clawson, J. (1998). High performance, gravity insensitive, enclosed aeroponic system for food production in space. *Principal Investigator, NASA SBIR NAS10-98030*.
- [Tessema et al.2017] Tessema, L., Chindi, A., W/Giorgis, G., Solomon, A., Shunka, E., and Seid, E. (2017). Determination of nutrient solutions for potato (*solanum tuberosum* l.) seed production under aeroponics production system. *De Gruyter Open*.
- [Towler et al.2008] Towler, M. J., Kim, Y., Wyslouzil, B. E., Correll, M. J., and Weathers, P. J. (2008). Design, development, and applications of

mist bioreactors for micropropagation and hairy root culture. *Plant Tissue Culture Engineering, Springer.*